ADVANCED FUNCTIONAL MATERIALS
www.afm-journal.de

Systematic Investigation of Side-Chain Branching Position Effect on Electron Carrier Mobility in Conjugated Polymers

Jin-Hu Dou, Yu-Qing Zheng, Ting Lei, Shi-Ding Zhang, Zhi Wang, Wen-Bin Zhang, Jie-Yu Wang, and Jian Pei**

Recently, polymer field-effect transistors have gone through rapid development. Nevertheless, charge transport mechanism and structure-property relationship are less understood. Here we use strong electron-deficient benzodifurandione-based poly(*p*-phenylene vinylene) (BDPPV) as polymer backbone and develop six BDPPV-based polymers (BDPPV-C1 to C6) with various side-chain branching positions to systematically study the side-chain effect on device performance. All the polymers exhibited ambient-stable *n*-type transporting behaviors with the highest electron mobility of up to 1.40 $cm^2 V^{-1} s^{-1}$. The film morphologies and microstructures of all the six polymers were systematically investigated. Our results demonstrate that the interchain π–π stacking distance decreases as moving the branching position away from polymer backbones, and an unprecedentedly close π–π stacking distance down to 3.38 Å is obtained for BDPPV-C4 to C6. Nonetheless, closer π–π stacking distance does not always correlate with higher electron mobility. Polymer crystallinity, thin film disorder, and polymer packing conformation, which all influenced by side-chain branching position, are proved to show significant influence on device performance. Our study not only reveals that π–π stacking distance is not the decisive factor on carrier mobility in conjugated polymers but also demonstrates that side-chain branching position engineering is a powerful strategy to modulate and balance these factors in conjugated polymers.

1. Introduction

Conjugated polymers have been gaining their popularity in low-cost, flexible, and large-area electronic applications due to their excellent solution-processability, good mechanical property, and the ease of tuning their electronic properties.[1–7] In the past few years, considerable efforts have been devoted to the development of novel building blocks, such as benzothiadiazole (BT),[8,9] diketopyrrolopyrrole (DPP),[10–14] isoindigo (II),[15–18] naphthalene diimide (NDI),[19,20] benzobisthiadiazole (BBT),[21,22] and benzodifurandione-based oligo(p-phenylene vinylene) (BDOPV),[23–26] which leads to significant progress in carrier mobilities of polymer semiconductors.[27] However, current polymer structure design is still based on try-and-error approach, and rational polymer design is largely limited by the less understanding of carrier transport mechanism and structure-property relationship.[28,29]

Solution-processable conjugated polymers generally contain conjugated backbones and flexible solubilizing side chains. To improve the device performance and investigate the structure-property relationship, most studies have focused on varying the backbone structures.[30,31] However, except for the difficulties in the synthesis of new building blocks and obtaining backbones with excellent electronic properties, significant structural changes in polymer backbone also lead to the difficulty in distinguishing the exact effect of each factor on carrier mobility, because both electronic properties and film microstructures will be changed by varying the backbone structures, making the study on structure-property relationship more complicated.[29,32] Side chains of conjugated polymers, often regarded as solubilizing groups, are recently found to have substantial impacts on film microstructure and device performance.[33,34] Compared with the backbone structure manipulation, "side-chain engineering" strategy can avoid the time-consuming backbone synthesis and achieve the fine tuning of device performance.[35–39] In addition, because of the less structural changes in engineering side-chains, this strategy provides a straightforward approach to investigate the structure-property relationship and has been widely used in both small molecules and polymer semiconductors.[31,40,41]

Although branched alkyl chains provide good solubility for conjugated polymers, the large van der Waals radii between alkyl side chains may hinder the interchain π–π stacking of conjugated polymers.[18,42] To avoid this problem, Bao et al. designed a siloxane-terminated side chain and significantly boosted the mobility of isoindigo-based polymer. They

J.-H. Dou, Y.-Q. Zheng, T. Lei, S.-D. Zhang, Z. Wang, Prof. W.-B. Zhang, Dr. J.-Y. Wang, Prof. J. Pei
Beijing National Laboratory for Molecular Sciences
The Key Laboratory of Bioorganic Chemistry and Molecular Engineering of Ministry of Education
Center of Soft Matter Science and Engineering
College of Chemistry and Molecular Engineering
Peking University
Beijing 100871, China
E-mail: jieyuwang@pku.edu.cn; jianpei@pku.edu.cn

DOI: 10.1002/adfm.201401822

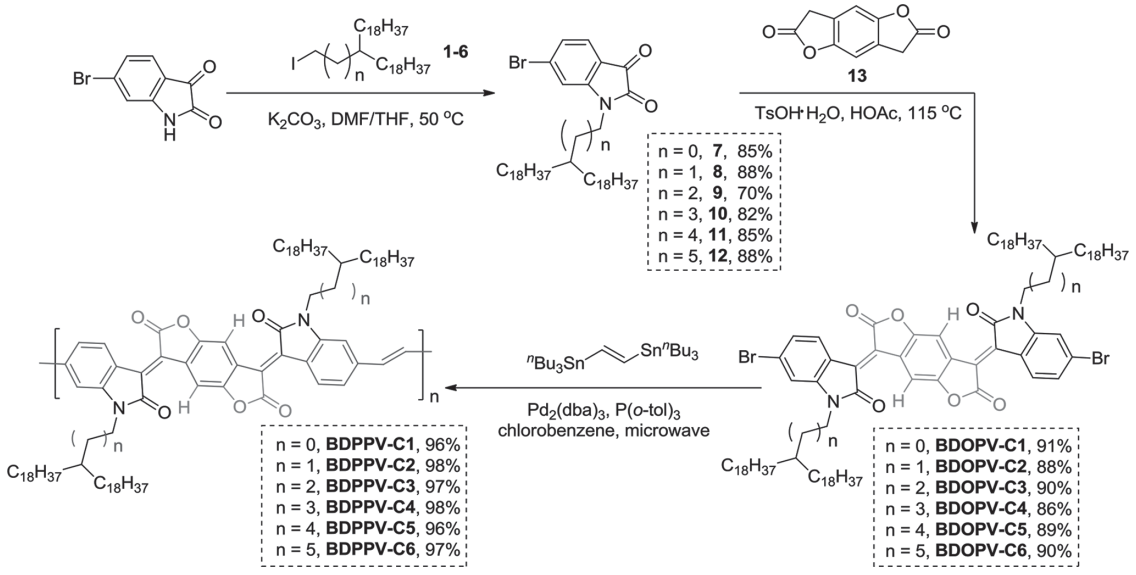

Scheme 1. The synthetic route to **BDOPV** monomers and **BDPPV** polymers with alkyl side chains branched at different positions.

proposed that the decrease of π–π stacking distance is a key factor to achieve high carrier mobility in conjugated polymers.[16] Because of the poor stability of trimethylsilyl groups and their limited solubility for large conjugated backbones, we and several other groups designed "more conventional" alkyl chains with different branching positions, and significantly improved the carrier mobility of different types of conjugated polymers.[11,12,43,44] In these studies, the improvement of the carrier mobility was largely explained by the closer π–π stacking distance. However, systematic studies on side-chain branching positions are seldom conducted, and other effects beyond decreasing π–π stacking distance have not been revealed yet. Furthermore, the influence of alkyl-chain branching positions on *n*-type conjugated polymers has not been examined.

Herein, to systematically study the branching position effects, we choose strong electron-withdrawing benzodifurandione-based poly(*p*-phenylene vinylene) (**BDPPV**) as polymer backbone and gradually move the branching position of side chains, and finally develop six polymers, **BDPPV-C1**, **BDPPV-C2**, **BDPPV-C3**, **BDPPV-C4**, **BDPPV-C5**, and **BDPPV-C6** (**Scheme 1**). All the six polymers exhibit ambient-stable *n*-type transporting behaviors with high electron mobility of up to 1.40 $cm^2\ V^{-1}\ s^{-1}$. Systematic studies show that the interchain π–π stacking distance decreases as moving the branching position away from polymer backbones, and an unprecedentedly close π–π stacking distance down to 3.38 Å is obtained, which is probably the smallest π–π stacking distance reported in conjugated polymers.[16,25] However, smaller π–π stacking distance does not provide higher carrier mobility. Our results reveal that π–π stacking distance does not have decisive impact on carrier mobility. A subtle variation in side-chain structure can exert great influence on polymer crystallinity, thin film disorder, and polymer packing conformation, and device performance is determined by all the factors.

2. Results and Discussion

2.1. Design Strategy and Synthesis

BDPPV was chosen as the polymer backbone due to its low-lying lowest unoccupied molecular orbital (LUMO) level around −4.0 eV and shape-persistent structure, thus high-performance *n*-type transport is anticipated.[24] Scheme 1 illustrates the synthetic route to six **BDPPV** derivatives. Six novel branched side chains (for compounds **1** to **6**), 2-octadecyleicosyl, 3-octadecylheneicosyl, 4-octadecyldocosyl, 5-octadecyltricosyl, 6-octadecyltetracosyl, 7-octadecylpentacosyl, were used.[43] The branching positions of the side chains were moved gradually away from the polymer backbones.

The synthesis started from the *N*-alkylation of commercially available 6-bromoisatin, giving **7** to **12** in good yields under basic conditions. Subsequently, by using acidic condensation condition between **7** to **12** and benzo[1,2-*b*:4,5-*b'*]difuran-2,6(3*H*,7*H*)-dione (**13**), six **BDOPV** monomers were obtained with high yields. Interestingly, the R_f values of **BDOPV-C4** (0.40), **BDOPV-C5** (0.40) and **BDOPV-C6** (0.41) from thin layer chromatography (TLC) are significantly smaller than those of **BDOPV-C1** (0.50), **BDOPV-C2** (0.50) and **BDOPV-C3** (0.49) (Figure S1). A possible explanation to this phenomenon might be the shielding effects of the farther branched alkyl chains are weakened and the polar groups, such as amide, are more exposed after moving the branching position away from the backbone, thus leading to the stronger interactions between the monomers and silica gel. Microwave-assisted Stille coupling polymerizations using (*E*)-1,2-bis-(tributylstannyl)ethene generated six target polymers, named **BDPPV-C1**, **BDPPV-C2**, **BDPPV-C3**, **BDPPV-C4**, **BDPPV-C5**, and **BDPPV-C6**, respectively. Notice that these polymers exhibit good solubility in common organic solvents, such as chloroform and *o*-dichlorobenzene (ODCB), due to the long alkyl chains. In order to exclude the impact of molecular weight, careful control of the

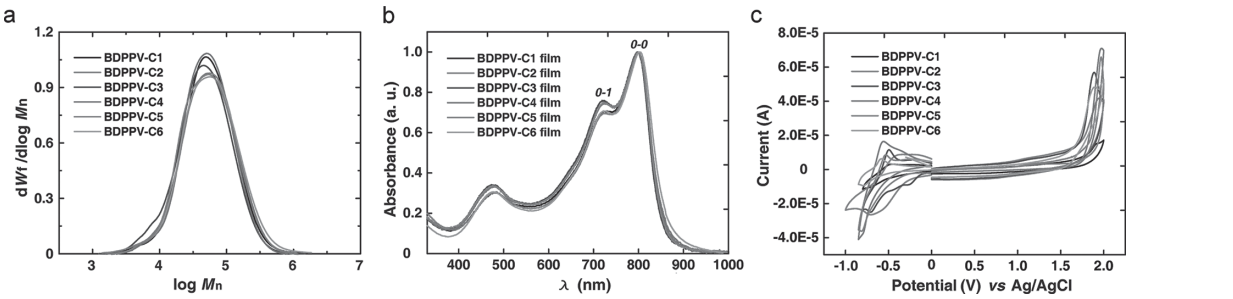

Figure 1. a) Gel permeation chromatography (GPC) traces of six polymers. Molecular weights were evaluated with 1,2,4-trichlorobenzene as eluent at 150 °C. b) Normalized absorption spectra of their pristine films spin-coated from chloroform solution (1 mg/mL). c) Cyclic voltammograms of six polymers in thin films drop-casted on glassy carbon electrode and tested in *n*-Bu_4NPF_6/CH_3CN solution (scan rate: 50 mV s^{-1}).

polymerization process was realized and six polymers with very close number-average molecular weights (M_n) and polydispersity (PDI) were obtained (**Figure 1**a, Figure S2 and **Table 1**). The molecular weights of six polymers were evaluated by high-temperature gel permeation chromatography (GPC) at 150 °C using polystyrenes as standards and 1,2,4-trichlorobenzene (TCB) as eluent. All the polymers show good thermal stability with decomposition temperatures over 370 °C (Figure S3).

2.2. Photophysical and Electrochemical Properties

The absorption spectra of the six polymers both in dilute solution and in thin film were characterized. The absorption spectra of the six monomers (**BDOPV-C1** to **C6**) were almost the same due to their identical backbone structures (Figure S4a). However, the six polymers showed similar but slightly different UV-*vis* absorption spectra with low optical bandgaps around 1.44 eV (Figure 1b, Figure S4b, and Figure S4c). In the film absorption spectra, no obvious spectral shift was observed for six polymers compared to those in dilute solution, indicating that the polymers might form some pre-aggregates in solution due to their strong intermolecular interactions (Figure S4d-i).[45,46] A close examination of the absorption peaks around 800 nm revealed an obvious difference in the relative intensity of *0–0* and *0–1* vibrational peaks among six polymers both in dilute solution and in thin film, suggesting that these polymers formed different aggregation states from each other (Figure 1b and Figure S4b).[47] On the other hand, an increase of the relative intensity of *0–0* vibrational peaks from solution to films was observed for all the six polymers, suggesting that the aggregation state of each polymer in solution was different from that in film. Annealing the films resulted in further increase of the relative intensity of *0–0* vibrational peaks, suggesting that annealing might be useful for further adjustment in film.

Cyclic voltammetry (CV) was performed to evaluate electrochemical properties of the six polymers in thin film (Figure 1c). The six polymers showed similar highest occupied molecular orbital (HOMO) and LUMO levels. All the polymers showed low-lying LUMO levels (from -3.97 to -4.07 eV), lower than those of several ambient-stable *n*-type polymers, which indicates that the polymers may be suitable for ambient-stable electron transport (Table 1).[48–50] Similar HOMO and LUMO energy levels proved that the incorporation of branched alkyl chains did not significantly change the electrochemical properties of the polymers. Photoelectron spectroscopy (PES) was also used to measure the HOMO energy levels of all polymers, which displayed consistent results (Figure S6 and Table 1).

2.3. Fabrication and Performance of Solution-processed FETs

Top-gate/bottom-contact (TG/BC) device structure was used to fabricate the FET devices of these polymers due to its better injection characteristics and encapsulation effects.[19] Solutions of the six polymers in ODCB (3 mg/mL) prepared by stirring at 100 °C overnight were spin-coated onto Au-patterned Si/SiO_2 substrates. CYTOP was used as dielectric layer in the fabrication of TG/BC devices through spin-coating, and Al electrode of 80 nm was evaporated thereon under high vacuum

Table 1. Summary of Optical and Electrochemical Properties of Six Polymers.

Polymers	M_n [kDa]/PDI[a)]	T_d/T_m [°C]	λ_{max} [nm] sol[b)]	λ_{max} film [nm]	E_g^{opt} [eV][c)]	E_{HOMO} [eV][d)]	E_{LUMO} [eV][d)]	E_g^{cv} [eV][e)]	E_{HOMO}^{PES} [eV]
BDPPV-C1	37.4/2.04	378/27.0	795, 726	800, 730	1.44	–6.16	–4.01	2.15	–5.92
BDPPV-C2	37.7/2.26	381/24.9	797, 726	800, 727	1.44	–6.15	–4.07	2.08	–5.90
BDPPV-C3	30.2/2.25	376/26.8	799, 723	800, 724	1.45	–6.16	–4.01	2.15	–5.76
BDPPV-C4	34.9/2.01	378/26.4	799, 728	800, 723	1.43	–6.15	–3.97	2.18	–5.78
BDPPV-C5	35.9/2.26	382/28.0	799, 727	800, 722	1.45	–6.16	–4.02	2.14	–5.78
BDPPV-C6	35.2/2.44	382/32.7	803, 725	803, 723	1.44	–6.12	–4.01	2.11	–5.78

[a)]Molecular weights of all polymers were evaluated by gel permeation chromatography (GPC) using 1,2,4-trichlorobenzene (TCB) as eluent at 150 °C; [b)]10^{-5} M in chloroform; [c)]Estimated from the onset of thin-film absorption; [d] Cyclic voltammetry determined with Fc/Fc^+ (E_{HOMO} = –4.80 eV) as external reference; [e] $E_g^{CV} = E_{LUMO} – E_{HOMO}$.

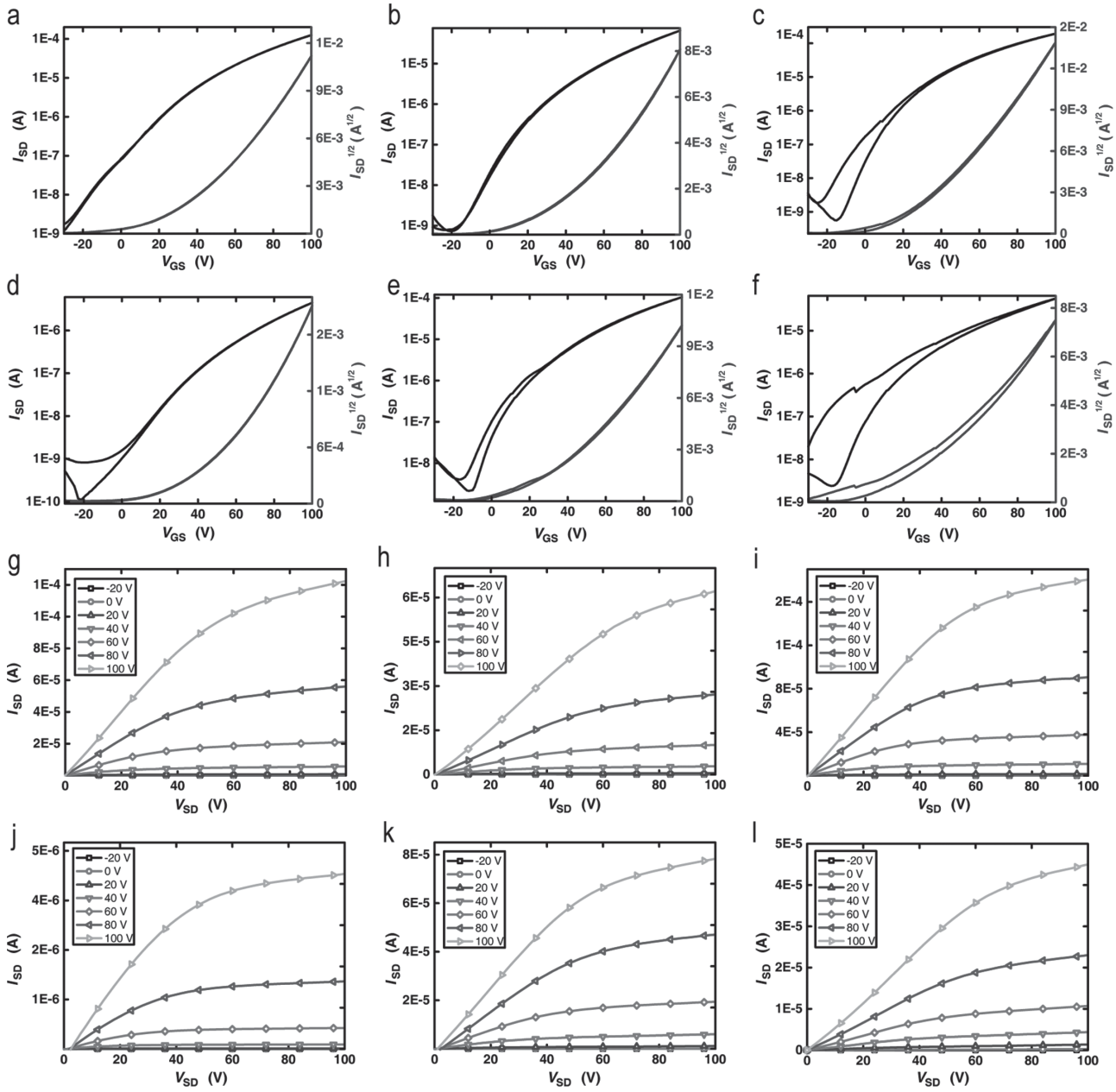

Figure 2. Transfer (up) and output (down) characteristics of the devices measured under ambient conditions. a, g) **BDPPV-C1**, b, h) **BDPPV-C2**, c, i), **BDPPV-C3**, d, j) **BDPPV-C4**, e, k) **BDPPV-C5**, and f, l) **BDPPV-C6** (films spin-casted from ODCB solutions, 3 mg/mL) at V_{SD} = 100 V (L = 5 μm, W = 100 μm, capacitance C_i = 3.7 nF cm^{-2}) after thermal annealing at 180 °C for 5 min.

(~1 × 10^{-5} Pa). As annealing process could facilitate planarization of polymer backbones in films, different annealing temperatures from 100 °C to 200 °C were applied for six polymers. The best device performance was obtained after annealing at 180 °C for all the polymers. All six polymers exhibited typical *n*-type transfer and output characteristics under ambient conditions (**Figure 2**, **Table 2**). The electron mobilities of all polymers did not change linearly as branching positions of alkyl chains moved away from the backbones, but showed fluctuation instead. With alkyl chains branched in odd-numbered positions, **BDPPV-C1**, **BDPPV-C3**, and **BDPPV-C5** showed relatively higher electron mobilities of 0.90 cm^2 V^{-1} s^{-1}, 1.40 cm^2 V^{-1} s^{-1}, 0.76 cm^2 V^{-1} s^{-1}, and the electron mobility of **BDPPV-C3** is among the highest in *n*-type conjugated polymers under ambient conditions.[19,50] Their statistic data followed the same trend as their highest electron mobilities (Figure S7), By contrast, with alkyl chains branched in even-numbered positions, **BDPPV-C4** showed only two orders of magnitude lower mobility of 0.05 cm^2 V^{-1} s^{-1}, and **BDPPV-C6** showed the highest mobility of 0.44 cm^2 V^{-1} s^{-1}, obviously lower than other three polymers. As to the threshold voltage, odd-even effect was also observed for **BDPPV-C1** to **C6**. Polymers with alkyl chains branched at odd-numbered positions exhibited statistically smaller threshold voltage at around 36 V, while **BDPPV-**

Table 2. Summary of OFET Device Performance and GIWAXS Results of Six Polymers.

Polymers	$T_{annealing}$ [°C]	μ [cm^2 V^{-1} s^{-1}][a]	V_T [V][b]	I_{on}/I_{off}	d [Å][c]	
					L	π
BDPPV-C1	180	0.90 (0.73)	38 (36)	>10^5	30.2	3.52
BDPPV-C2	180	0.60 (0.38)	52 (44)	>10^4	32.2	3.48
BDPPV-C3	180	1.40 (1.12)	36 (35)	>10^5	33.8	3.45
BDPPV-C4	180	0.05 (0.03)	49 (54)	>10^4	36.6	3.38
BDPPV-C5	180	0.76 (0.65)	39 (37)	>10^5	39.5	3.38
BDPPV-C6	180	0.44 (0.33)	41 (41)	>10^3	41.3	3.38

[a]Electron mobilities measured under ambient conditions (R_H = 50–60%). Maximum values of electron mobilities and the average values are in parentheses; [b]Corresponding values of threshold voltage and the average values are in parentheses; [c]Lamellar (L) and π–π stacking (π) distances were determined by GIWAXS experiments.

C2 and **C4** showed much higher threshold voltages at around 50 V. Time-dependent decays of the device performance were tested by storing the devices under ambient conditions (R_H = 50–60%). All polymers showed good air-stability with a slow decrease of electron mobility. **BDPPV-C5** remained 40% electron mobility after being stored for over 20 days (Figure S8), which surpasses many *n*-type conjugated polymers.[19,50,51] Although there are only tiny differences in the structure of six polymers, they exhibited distinct electron mobilities after an identical fabrication process. These results suggest that a subtle change of alkyl side chains in conjugated polymers can lead to significant difference in device performance, which arouse our interest in the investigation of the structure-property relationship in these conjugated polymers.

2.4. Film Morphology and Microstructural Analysis

Tapping-mode atomic force microscopy (AFM), grazing incident wide-angle X-ray scattering (GIWAXS) and grazing incident small-angle X-ray scattering (GISAXS) were used to analyze film morphology and microstructure of each polymer film.[52] Films were prepared by spin-coating the polymer solutions on electrode-free Si/SiO_2 substrates and then annealed under the same condition as the device fabrication. From AFM height images, it was observed that all the polymer films showed nanofibrillar intercalated structures with obvious crystallized domains (**Figure 3**, phase images in Figure S9). The strong crystallization capability of **BDPPV-C1** to **BDPPV-C6** may contribute to their high electron mobilities. All the polymer films showed close root-mean-square (RMS) roughness of 1.07, 0.99, 1.13, 1.21, 1.35, 0.93 nm, respectively. Similar surface roughness can guarantee similar contact with the CYTOP dielectric layer, thus the difference in electron mobility was not caused by contact problem between the active and the dielectric layers.

In the GIWAXS patterns, all the polymer films showed strong out-of-plane diffraction peaks along the q_z axis, indexed as (h00) and in-plane diffraction partial arcs along q_{xy} axis (q ~ 1.8 Å^{-1}), indexed as (010). The two sets of diffractions are assigned to lamellar packing and π–π stacking, respectively (**Figure 4**). These diffraction patterns indicate that a typical edge-on packing mode with π-plane perpendicular to the substrates and π–π stacking direction parallel to the substrates are formed in films.[53] However, in **BDPPV-C1**, **BDPPV-C2**, **BDPPV-C3** and **BDPPV-C4** patterns, π–π stacking diffractions along the q_z axis were also observed, indicating the co-existence of face-on packing mode, whereas **BDPPV-C5** and **BDPPV-C6** did not show diffraction peaks assigned to face-on packing. Lamellar distances of the polymers extended from 30.2 to 41.3 Å as the

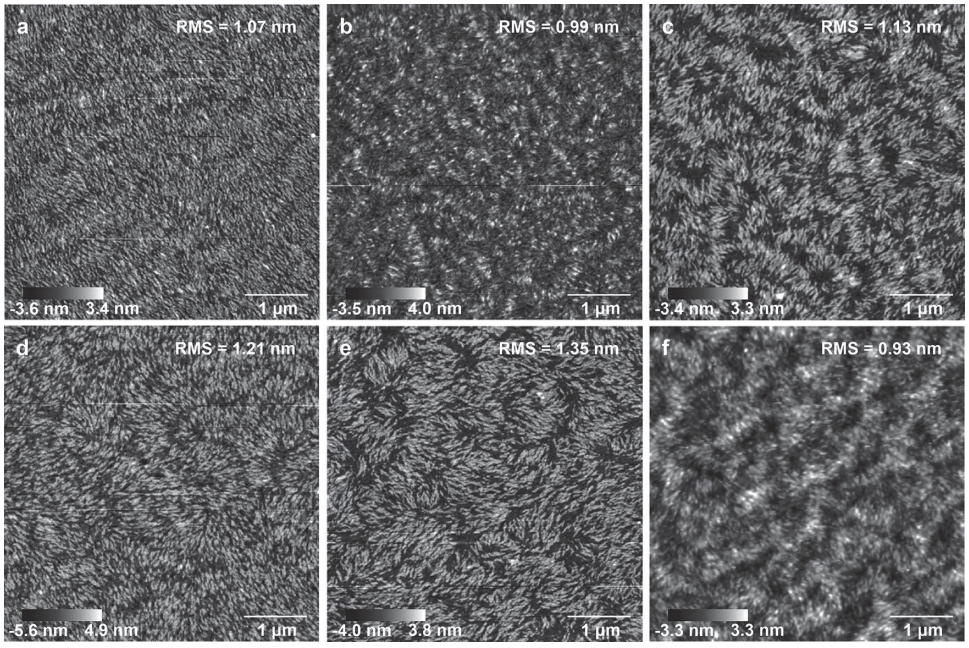

Figure 3. Tapping-mode AFM height images of a) **BDPPV-C1**, b) **BDPPV-C2**, c) **BDPPV-C3**, d) **BDPPV-C4**, e) **BDPPV-C5**, and f) **BDPPV-C6** films prepared by spin-coating their ODCB solutions (3 mg/mL) and annealing at 180 °C for 30 min. The scope of the AFM images is 5 mm.

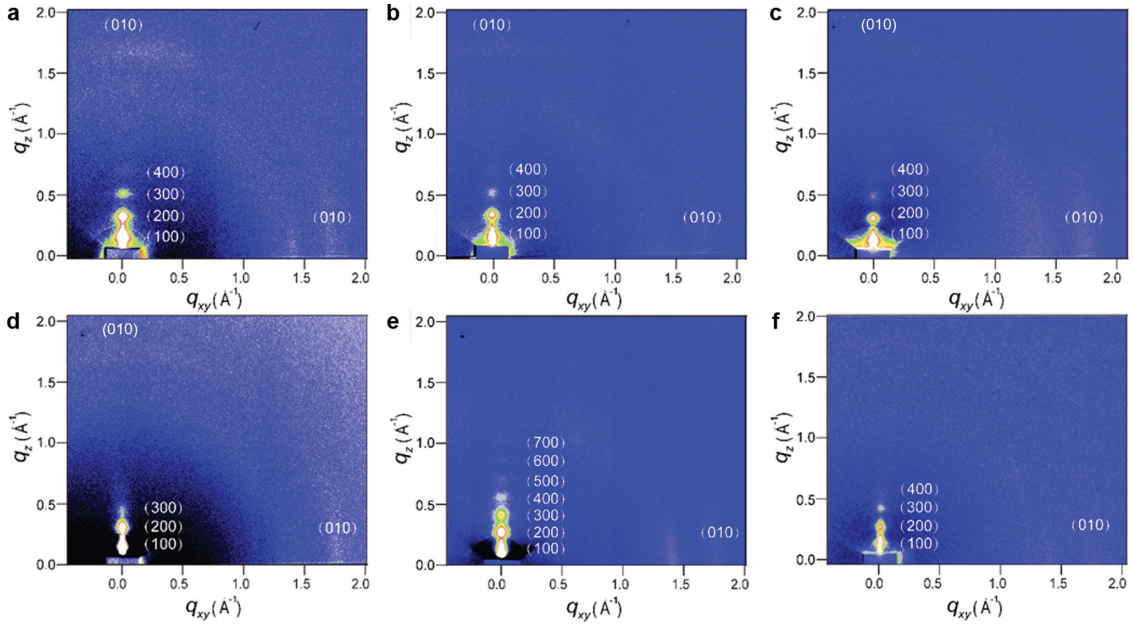

Figure 4. 2D-GIWAXS patterns of a) **BDPPV-C1**, b) **BDPPV-C2**, c) **BDPPV-C3**, d) **BDPPV-C4**, e) **BDPPV-C5,** and f) **BDPPV-C6** films prepared by spin-coating their DCB solutions (3 mg/mL) and annealed at 180 °C for 30 min.

total length of the alkyl chains increasing. Meanwhile, as the branching positions moving away from the backbone, π–π stacking distance decreased from 3.52 Å for **BDPPV-C1** to 3.45 Å for **BDPPV-C3** and became unchanged for **BDPPV-C4**, **BDPPV-C5** and **BDPPV-C6** (3.38 Å) (Table 2). Note that 3.38 Å is significantly shorter than other high-performance conjugated polymers, which is probably the shortest π–π stacking distance reported in conjugated polymers.[8,11,12,15,19,21,24] The gradual decrease of π–π distance benefits from farther branched alkyl chains, which can reduce the steric hindrance from the branching position.[11,12,16]

Careful examination and analysis of the 2D-GIWAXS patterns suggest that modulating the branching positions may result in different film disorders even under identical π–π stacking distance (Figure 4d, e and f). For example, **BDPPV-C5** film displayed seven out-of-plane diffraction peaks, whereas **BDPPV-C6** film showed four out-of diffraction peaks and **BDPPV-C4** film showed only three. This indicates that **BDPPV-C5** film has more ordered lamellar packing than **BDPPV-C6** and **BDPPV-C4** films. The less ordered film of **BDPPV-C4** indicates the chaos of the polymer packing, which might corrupt the transport path and thereby lower the carrier mobility.[54,55]

To gain more information about the ordering and preferential orientations of the domains in polymer films, GISAXS characterization of the polymer films were performed, and the scattering experiment details are described in the Supporting Information. To well separate film scattering peaks from both reflected beam of the substrates and Yoneda peaks of the polymers, we chose an incident angle of $\alpha_i = 0.4°$ (**Figure 5**). GISAXS images of all polymer films showed a diffuse Bragg sheet along q_z direction (~0.065 Å^{-1}), while they showed no diffuse Bragg rods along q_y direction. This result indicates that the lamellar stacking of crystallized domains parallel to the substrate were formed in film (Figure S11 and Figure S12).[56] Using the distorted-wave Born approximation,[57] the thickness of the lamellar crystal domains could be calculated (Figure S11). All six polymers showed lamellar domain thickness of 96.7, 97.3,

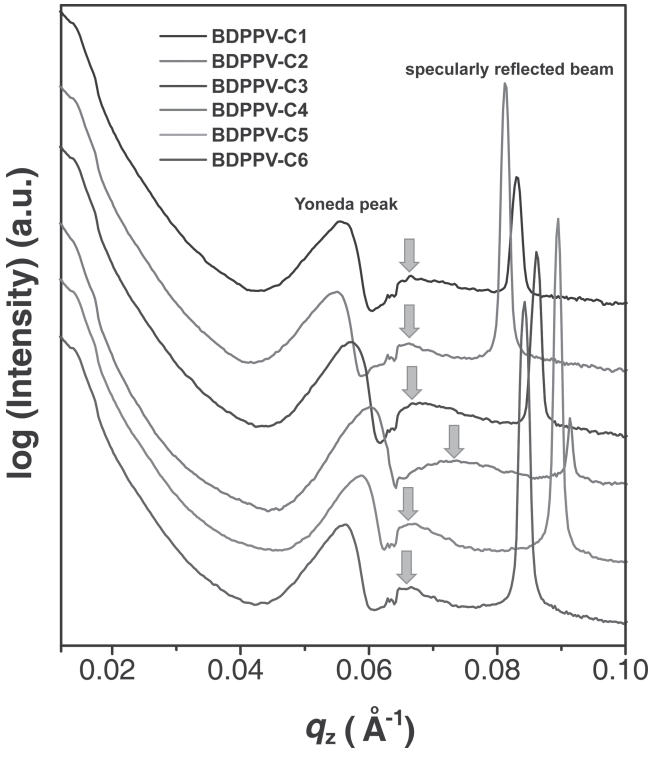

Figure 5. GISAXS patterns acquired for six polymer films with offset vertically for clarity. Yellow arrows indicate the first order diffuse Bragg sheet, more technical details and calculation methods seeing the Supporting Information.

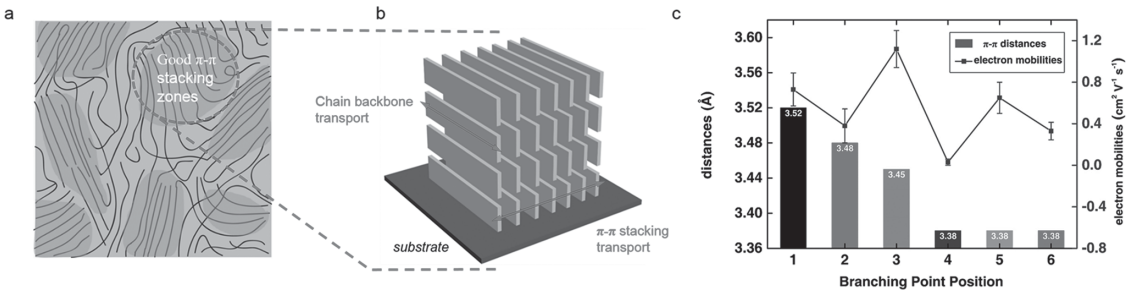

Figure 6. a) Schematics of the microstructure of a conjugated polymer film; b) Models of edge-on packing observed for conjugated polymers in good π–π stacking zones; c) Average electron mobilities (point) with error bars and π–π distance (histogram) of six polymers. Clear odd-even trend with side-chain branching position was observed.

95.2, 86.0, 96.4, and 97.6 Å, respectively. **BDPPV-C4** had the smallest domain thickness, indicating that it lacks long-range order and good crystallinity in film, which is consistent with GIWAXS data. The GISAXS diffraction peaks at 0.06–0.07 $Å^{-1}$ of **BDPPV-C4** were broad with low intensity when comparing with other five polymers, indicating the broad range of the sizes of crystalline domains of **BDPPV-C4** film.

3. Effects of Branching Position Engineering

Charge transport in conjugated polymer films is determined by intrachain and interchain transport (**Figure 6**a).[29,58–60] Generally, intrachain transport is determined by the polymer backbone properties, including electronic structures, effective conjugation length, and molecular weight. In our system, the polymers have the identical backbone and very close molecular weights and distributions. Therefore, we hypothesize that the differences in polymer mobilities mainly come from the interchain transport.

Bao et al. first reported that closer π–π distance can increase hole mobility in conjugated polymers.[16] We also found that gradually moving the branching position away from polymer backbone could gradually decrease π–π stacking distances and lead to an increase of hole mobility.[43] Recently, Kim et al. reported diketopyrrolopyrrole (DPP)-based polymers with alkyl chains of six methylene spacers exhibited unprecedented high hole mobilities of up to 12 $cm^2\ V^{-1}\ s^{-1}$.[12] The authors again attributed the much improved carrier mobilities to smaller π–π stacking distance. It seems that decreasing π–π distance can generally lead to increased carrier mobility in conjugated polymers. However, as we gradually moved the branching position of side chains away from backbone structure, gradual decrease in π–π stacking distance was realized, but the mobility does not correlate well with the π–π stacking distance and the shortest π–π distance does not necessarily render the highest electron mobility. For example, **BDPPV-C4** with the smallest π–π distance (3.38 Å), showed the lowest electron mobility, even lower than that of **BDPPV-C1** with the largest π–π distance (3.52 Å). In addition, although **BDPPV-C4** and **BDPPV-C5** showed the same π–π distance in film, the electron mobility of **BDPPV-C5** (0.76 $cm^2\ V^{-1}\ s^{-1}$) was over ten times higher than that of **BDPPV-C4** (0.05 $cm^2\ V^{-1}\ s^{-1}$). The unexpected results suggest that there must be other factors that determine the device performance.

In the GIWAXS, some polymers showed obviously higher molecular order in thin films. For example, **BDPPV-C5** film displayed seven orders of out-of-plane diffractions whereas **BDPPV-C4** only displayed three orders. Furthermore, GISAXS showed that **BDPPV-C4** showed less crystallinity in film, and its crystalline zones are smaller than other polymers. Therefore, we can conclude that besides modulating π–π stacking distance, side-chain branching position also influences thin film disorder and polymer crystallinity. Compared with **BDPPV-C3**, **BDPPV-C5** have smaller π–π distance (3.38 Å) and higher molecular order in thin films. Unfortunately, **BDPPV-C5** (0.76 $cm^2\ V^{-1}\ s^{-1}$) showed lower electron mobility than **BDPPV-C3** (1.40 $cm^2\ V^{-1}\ s^{-1}$), even lower than that of **BDPPV-C1** (0.90 $cm^2\ V^{-1}\ s^{-1}$) with the largest π–π distance (3.52 Å). In the GISAXS characterization, the above three polymers have similar crystallinity. As we know, another important factor that determine the interchain transport is polymer interchain packing conformation. With the variation of branching position, the packing conformation between the adjacent polymer backbones might change, resulting in different interchain electronic coupling and electron mobility. We propose that **BDPPV-C3** may have a more appropriate interchain packing conformation and more efficient interchain electron transport than **BDPPV-C5**, though the π–π stacking distance of **BDPPV-C3** is larger. Theoretical calculation by Beljonne et al. have revealed that subtle changes on polymer packing conformations can alter the electronic coupling between polymer chains, thus significantly changing the charge transfer integral between polymer chains and affecting interchain transport.[61] In addition, a recent study by Patil et al. reported the single crystal structures of several DPP derivatives functionalized with linear and branched alkyl chains. They found that compared with linear alkyl chains, branched alkyl chains led to improper overlaps of the aromatic molecular backbones, which may be caused by steric hindrance effect of the branching positions.[42] Thus, we propose that the changes in branching positions may also affect polymer packing conformations and therefore carrier mobility.

Here we also observed interesting odd-even effect in electron mobility. It is very challenging to clarify the origin of the odd-even effect due to the great difficulty in determining the exact molecular packing of conjugated polymers. Because we did not observe any odd-even effect in π–π stacking distance, thin-film disorder and crystallinity of the polymer films, we propose that the different interchain packing conformations that caused by the different alkyl chain conformations of the six polymers might account for the odd-even effect. This was supported by our study on the alkyl chain effects in small-molecule organic

semiconductors.[62] We found that the odd-even effects of alkyl side chains was mainly caused by the different zig-zag conformation of alkyl chains. Alkyl chains tend to have all-*trans* conformation in solid state,[63] which may exert influences on interchain packing conformation and interchain electron transport.

4. Conclusion

In summary, we have developed six *n*-type **BDPPV**-based polymers with alkyl chains branched at different positions to systematically study the influence of the branching position on device performance, film morphology and polymer packing. All the polymers exhibited ambient-stable electron transport behaviors with the highest electron mobility of up to 1.40 $cm^2 V^{-1} s^{-1}$, which is among the highest electron mobilities of *n*-type polymer FETs. Systematic studies show that the interchain π–π stacking distance decreases as moving the branching position away from polymer backbones. We obtained an unprecedentedly close π–π stacking distance of 3.38 Å, probably the smallest π–π stacking distance in conjugated polymers. Previous studies indicate that smaller π–π stacking distance usually leads to higher carrier mobility in conjugated polymers. However, we find that π–π stacking distance does not correlate well with carrier mobility. We propose that besides π–π stacking distance, polymer crystallinity, thin film disorder, and polymer packing conformation might also have significant effect on device performance, and these factors can be finely modulated through engineering the side chain branching positions. Our study demonstrates that branching position engineering is a powerful tool to finely modulate the carrier transport in conjugated polymers and its effects are far beyond π–π distance modulation.

Supporting Information

Supporting Information is available from the Wiley Online Library or from the author.

Acknowledgements

This work was supported by the Major State Basic Research Development Program (2013CB933501) from the Ministry of Science and Technology, and National Natural Science Foundation of China. The authors thank beamlines BL14B1 and BL16B1 (Shanghai Synchrotron Radiation Facility) for providing the beam time.

Received: June 4, 2014
Revised: July 1, 2014
Published online: August 19, 2014

[1] A. J. Heeger, *Chem. Soc. Rev.* **2010**, *39*, 2354.
[2] J. H. Burroughes, D. D. C. Bradley, A. R. Brown, R. N. Marks, K. Mackay, R. H. Friend, P. L. Burns, A. B. Holmes, *Nature* **1990**, *347*, 539.
[3] Z. He, C. Zhong, S. Su, M. Xu, H. Wu, Y. Cao, *Nat. Photon.* **2012**, *6*, 593.
[4] C. V. Hoven, R. Yang, A. Garcia, V. Crockett, A. J. Heeger, G. C. Bazan, T. Q. Nguyen, *Proc. Natl. Acad. Sci. USA* **2008**, *105*, 12730.
[5] B. Sun, W. Hong, Z. Yan, H. Aziz, Y. Li, *Adv. Mater.* **2014**, *26*, 2636.
[6] J. B. You, L. T. Dou, K. Yoshimura, T. Kato, K. Ohya, T. Moriarty, K. Emery, C. C. Chen, J. Gao, G. Li, Y. Yang, *Nat. Commun.* **2013**, *4*, 1446.
[7] H. R. Tseng, H. Phan, C. Luo, M. Wang, L. A. Perez, S. N. Patel, L. Ying, E. J. Kramer, T. Q. Nguyen, G. C. Bazan, A. J. Heeger, *Adv. Mater.* **2014**, *26*, 2993.
[8] H. N. Tsao, D. M. Cho, I. Park, M. R. Hansen, A. Mavrinskiy, D. Y. Yoon, R. Graf, W. Pisula, H. W. Spiess, K. Müllen, *J. Am. Chem. Soc.* **2011**, *133*, 2605.
[9] H. R. Tseng, L. Ying, B. B. Hsu, L. A. Perez, C. J. Takacs, G. C. Bazan, A. J. Heeger, *Nano. Lett.* **2012**, *12*, 6353.
[10] C. B. Nielsen, M. Turbiez, I. McCulloch, *Adv. Mater.* **2013**, *25*, 1859.
[11] J. Lee, A. R. Han, H. Yu, T. J. Shin, C. Yang, J. H. Oh, *J. Am. Chem. Soc.* **2013**, *135*, 9540.
[12] I. Kang, H. J. Yun, D. S. Chung, S. K. Kwon, Y. H. Kim, *J. Am. Chem. Soc.* **2013**, *135*, 14896.
[13] J. Li, Y. Zhao, H. S. Tan, Y. Guo, C. A. Di, G. Yu, Y. Liu, M. Lin, S. H. Lim, Y. Zhou, H. Su, B. S. Ong, *Sci. Rep.* **2012**, *2*, 754.
[14] C. Kanimozhi, N. Yaacobi-Gross, K. W. Chou, A. Amassian, T. D. Anthopoulos, S. Patil, *J. Am. Chem. Soc.* **2012**, *134*, 16532.
[15] R. Stalder, J. Mei, K. R. Graham, L. A. Estrada, J. R. Reynolds, *Chem. Mater.* **2014**, *26*, 664.
[16] J. Mei, D. H. Kim, A. L. Ayzner, M. F. Toney, Z. Bao, *J. Am. Chem. Soc.* **2011**, *133*, 20130.
[17] T. Lei, Y. Cao, Y. Fan, C. J. Liu, S. C. Yuan, J. Pei, *J. Am. Chem. Soc.* **2011**, *133*, 6099.
[18] T. Lei, J.-Y. Wang, J. Pei, *Acc. Chem. Res.* **2014**, *47*, 1117.
[19] H. Yan, Z. Chen, Y. Zheng, C. Newman, J. R. Quinn, F. Dötz, M. Kastler, A. Facchetti, *Nature* **2009**, *457*, 679.
[20] X. Zhan, A. Facchetti, S. Barlow, T. J. Marks, M. A. Ratner, M. R. Wasielewski, S. R. Marder, *Adv. Mater.* **2011**, *23*, 268.
[21] J. Fan, J. D. Yuen, W. Cui, J. Seifter, A. R. Mohebbi, M. Wang, H. Zhou, A. Heeger, F. Wudl, *Adv. Mater.* **2012**, *24*, 6164.
[22] J. D. Yuen, J. Fan, J. Seifter, B. Lim, R. Hufschmid, A. J. Heeger, F. Wudl, *J. Am. Chem. Soc.* **2011**, *133*, 20799.
[23] T. Lei, J.-H. Dou, X.-Y. Cao, J.-Y. Wang, J. Pei, *Adv. Mater.* **2013**, *25*, 6589.
[24] T. Lei, J.-H. Dou, X.-Y. Cao, J.-Y. Wang, J. Pei, *J. Am. Chem. Soc.* **2013**, *135*, 12168.
[25] T. Lei, X. Xia, J.-Y. Wang, C. J. Liu, J. Pei, *J. Am. Chem. Soc.* **2014**, *136*, 2135.
[26] Z. Yan, B. Sun, Y. Li, *Chem. Commun.* **2013**, *49*, 3790.
[27] J. D. Yuen, F. Wudl, *Energy Environ. Sci.* **2013**, *6*, 392.
[28] C. Wang, H. Dong, W. Hu, Y. Liu, D. Zhu, *Chem. Rev.* **2012**, *112*, 2208.
[29] V. Coropceanu, J. Cornil, D. A. da Silva Filho, Y. Olivier, R. Silbey, J.-L. Brédas, *Chem. Rev.* **2007**, *107*, 926.
[30] J. Mei, Y. Diao, A. L. Appleton, L. Fang, Z. Bao, *J. Am. Chem. Soc.* **2013**, *135*, 6724.
[31] P. M. Beaujuge, J. M. Fréchet, *J. Am. Chem. Soc.* **2011**, *133*, 20009.
[32] J.-L. Brédas, D. Beljonne, V. Coropceanu, J. Cornil, *Chem. Rev.* **2004**, *104*, 4971.
[33] T. Lei, J.-Y. Wang, J. Pei, *Chem. Mater.* **2014**, *26*, 594.
[34] J. Mei, Z. Bao, *Chem. Mater.* **2014**, *26*, 604.
[35] C. Cabanetos, A. E. Labban, J. A. Bartelt, J. D. Douglas, W. R. Mateker, J. M. Fréchet, M. D. McGehee, P. M. Beaujuge, *J. Am. Chem. Soc.* **2013**, *135*, 4656.
[36] M. S. Chen, O. P. Lee, J. R. Niskala, A. T. Yiu, C. J. Tassone, K. Schmidt, P. M. Beaujuge, S. S. Onishi, M. F. Toney, A. Zettl, J. M. Fréchet, *J. Am. Chem. Soc.* **2013**, *135*, 19229.

[37] A. T. Yiu, P. M. Beaujuge, O. P. Lee, C. H. Woo, M. F. Toney, J. M. Fréchet, *J. Am. Chem. Soc.* **2012**, *134*, 2180.
[38] A. C. Mayer, M. F. Toney, S. R. Scully, J. Rivnay, C. J. Brabec, M. Scharber, M. Koppe, M. Heeney, I. McCulloch, M. D. McGehee, *Adv. Funct. Mater.* **2009**, *19*, 1173.
[39] S. Ko, E. T. Hoke, L. Pandey, S. Hong, R. Mondal, C. Risko, Y. Yi, R. Noriega, M. D. McGehee, J.-L. Brédas, A. Salleo, Z. Bao, *J. Am. Chem. Soc.* **2012**, *134*, 5222.
[40] B. Fu, J. Baltazar, A. R. Sankar, P.-H. Chu, S. Zhang, D. M. Collard, E. Reichmanis, *Adv. Funct. Mater.* **2014**, DOI: 10.1002/adfm.201304231.
[41] F. Zhang, Y. Hu, T. Schuettfort, C. A. Di, X. Gao, C. R. McNeill, L. Thomsen, S. C. Mannsfeld, W. Yuan, H. Sirringhaus, D. Zhu, *J. Am. Chem. Soc.* **2013**, *135*, 2338.
[42] M. A. Naik, N. Venkatramaiah, C. Kanimozhi, S. Patil, *J. Phys. Chem. C* **2012**, *116*, 26128.
[43] T. Lei, J.-H. Dou, J. Pei, *Adv. Mater.* **2012**, *24*, 6457.
[44] I. Meager, R. S. Ashraf, S. Mollinger, B. C. Schroeder, H. Bronstein, D. Beatrup, M. S. Vezie, T. Kirchartz, A. Salleo, J. Nelson, I. McCulloch, *J. Am. Chem. Soc.* **2013**, *135*, 11537.
[45] R. Steyrleuthner, M. Schubert, I. Howard, B. Klaumunzer, K. Schilling, Z. Chen, P. Saalfrank, F. Laquai, A. Facchetti, D. Neher, *J. Am. Chem. Soc.* **2012**, *134*, 18303.
[46] N. Zhou, X. Guo, R. P. Ortiz, S. Li, S. Zhang, R. P. Chang, A. Facchetti, T. J. Marks, *Adv. Mater.* **2012**, *24*, 2242.
[47] F. C. Spano, *Acc. Chem. Res.* **2010**, *43*, 429.
[48] Z. Chen, Y. Zheng, H. Yan, A. Facchetti, *J. Am. Chem. Soc.* **2009**, *131*, 8.
[49] Y. Takeda, T. L. Andrew, J. M. Lobez, A. J. Mork, T. M. Swager, *Angew. Chem., Int. Ed.* **2012**, *51*, 9042.
[50] H. Li, F. S. Kim, G. Ren, S. A. Jenekhe, *J. Am. Chem. Soc.* **2013**, *135*, 14920.
[51] J. K. Lee, M. C. Gwinner, R. Berger, C. Newby, R. Zentel, R. H. Friend, H. Sirringhaus, C. K. Ober, *J. Am. Chem. Soc.* **2011**, *133*, 9949.
[52] J. Rivnay, S. C. Mannsfeld, C. E. Miller, A. Salleo, M. F. Toney, *Chem. Rev.* **2012**, *112*, 5488.
[53] E. Cho, C. Risko, D. Kim, R. Gysel, N. C. Miller, D. W. Breiby, M. D. McGehee, M. F. Toney, R. J. Kline, J.-L. Brédas, *J. Am. Chem. Soc.* **2012**, *134*, 6177.
[54] R. Noriega, J. Rivnay, K. Vandewal, F. P. Koch, N. Stingelin, P. Smith, M. F. Toney, A. Salleo, *Nat. Mater.* **2013**, *12*, 1038.
[55] J. Rivnay, R. Noriega, R. J. Kline, A. Salleo, M. F. Toney, *Phys. Rev. B* **2011**, *84*, 045203.
[56] P. Busch, M. Rauscher, D. M. Smilgies, D. Posselt, C. M. Papadakis, *J. Appl. Cryst.* **2006**, *39*, 433.
[57] Z. Di, D. Posselt, D.-M. Smilgies, R. Li, M. Rauscher, I. I. Potemkin, C. M. Papadakis, *Macromolecules* **2012**, *45*, 5185.
[58] X. Feng, V. Marcon, W. Pisula, M. R. Hansen, J. Kirkpatrick, F. Grozema, D. Andrienko, K. Kremer, K. Müllen, *Nat. Mater.* **2009**, *8*, 421.
[59] A. A. Sagade, K. V. Rao, U. Mogera, S. J. George, A. Datta, G. U. Kulkarni, *Adv. Mater.* **2012**, *25*, 559.
[60] U. Mogera, A. A. Sagade, S. J. George, G. U. Kulkarni, *Sci. Rep.* **2014**, *4*, 4103.
[61] D. Niedzialek, V. Lemaur, D. Dudenko, J. Shu, M. R. Hansen, J. W. Andreasen, W. Pisula, K. Müllen, J. Cornil, D. Beljonne, *Adv. Mater.* **2013**, *25*, 1939.
[62] L. Ding, H.-B. Li, T. Lei, H.-Z. Ying, R.-B. Wang, Y. Zhou, Z.-M. Su, J. Pei, *Chem. Mater.* **2012**, *24*, 1944.
[63] R. Boese, H.-C. Weiss, D. Bläser, *Angew. Chem. Int. Ed.* **1999**, *38*, 988.